Journal of ELECTRONIC MATERIALS, Vol. 36, No. 12, 2007
DOI: 10.1007/s11664-007-0239-9

Regular Issue Paper

On the Nature of the Interface between Ag_3Sn Intermetallics and Sn in Sn-3.5Ag Solder Alloys

RAJEN S. SIDHU,[1] SHANTANU V. MADGE,[1,2] XIN DENG,[1,3] and NIKHILESH CHAWLA[1,4]

1.—School of Materials, Fulton School of Engineering, Arizona State University, Tempe, AZ 85287-8706, USA. 2.—*Present Address*: International Advanced Research Centre for Powder Metallurgy and New Materials, Hyderabad, India. 3.—*Present Address*: Kennametal Inc, Rogers, AK, USA. 4.—e-mail: nchawla@asu.edu

We report on the nature of the orientation of Ag_3Sn and the Ag_3Sn/Sn interface in Sn-3.5Ag solder. Orientation imaging microscopy (OIM) and transmission electron microscopy (TEM) were used to characterize the orientation and nature of the interface, respectively. OIM and TEM showed that Sn-3.5Ag containing spherical Ag_3Sn particles does not have a preferred orientation with respect to the Sn matrix. However, needle-like Ag_3Sn formed during slower cooling appeared to have a preferred orientation within individual Sn colonies. The interface between Sn and Ag_3Sn appeared to be incoherent, as confirmed by high-resolution TEM analysis.

Key words: Sn-rich solder, orientation image microscopy, transmission electron microscopy, Pb-free solder, Ag_3Sn

INTRODUCTION

Solders are used as interconnect materials in electronic packaging.[1–3] Traditionally, eutectic and near-eutectic Pb-Sn solder alloys have been used. Due to the toxicity and heath hazards associated with lead, Sn-rich (Pb-free) solders alloys are being considered for replacement of Pb-Sn. Among the potential lead-free solders, Sn-3.5Ag solder has been broadly targeted as a potential candidate for replacement of Pb-Sn solder. Sn-3.5Ag solder possesses excellent mechanical properties and improved high-temperature resistance compared to Pb-Sn.[1,4–6] The eutectic microstructure of the Sn-3.5Ag solder system consists of two phases: a Sn-rich matrix, and Ag_3Sn intermetallics that form from the reaction between Sn and Ag.[6–10]

The mechanical properties of solders are controlled by their microstructure, which depends strongly on solidification characteristics. Several investigations have been conducted on the microstructure and mechanical behavior of the Sn-3.5Ag alloy.[7–19] Ochoa et al.[6–8] showed that at very fast cooling rates (24°C/s) a combination of Sn dendrites and a fine eutectic mixture, consisting of a fine dispersion of Ag_3Sn particles in a Sn matrix, is formed. At slower cooling rates (0.1°C/s) a completely eutectic microstructure was formed, with the Ag_3Sn forming in needle-like form. Sidhu and Chawla[11,12] confirmed the needle-like nature of Ag_3Sn by three-dimensional visualization of the microstructure, using a serial sectioning technique. The fine dispersion of Ag_3Sn intermetallics within the solder has been shown to significantly improve the ultimate tensile strength and creep resistance of the alloy.[6–10] In fact, the creep resistance of Sn-3.5Ag solder has been shown to be controlled by the Ag_3Sn interparticle size and spacing, with the dominant deformation mechanisms being climb of dislocations over Ag_3Sn particles, as well as dislocation detachment from the particles.[13] In order to understand the dislocation interactions in this alloy system fully, the interface between the Sn-rich matrix and the Ag_3Sn particles needs to be characterized. Both the orientation relationship between particle/needle and matrix, and the degree of interface coherency between the Ag_3Sn particles and Sn-rich matrix (if any) will significantly affect the solder alloy's mechanical performance.

(Received June 20, 2007; accepted July 31, 2007; published online September 18, 2007)

Recently, several authors have examined the orientation of the Sn grain structure in Sn-rich solders using orientation imaging microscopy (OIM).[20–28] These authors have shown that solder joints similar to those found in electronic packages contain 5–20 grains along their length and relatively few Sn crystals across their thickness (typically one to three grains depending on the geometry and processing conditions).[22,23] Kumar et al.[26] conducted a study on Sn-Ag-Cu alloy using OIM, and established that increasing the processing temperature resulted in less texture and grain boundary orientations in the bulk solder. The authors attributed the increase in texture at lower reflow temperatures to the formation of solidification twins. Telang et al.[27,28] have determined that, during thermomechanical cycling, grain-boundary sliding is observed between grains that are misorientated by 7 or 14° as tilt boundaries about the [110] axes. In addition, preliminary work on the texture and orientation of Cu-Sn intermetallics at the solder/Cu substrate has been established,[26] showing that individual Cu_6Sn_5 nodules have a single orientation. Although extensive work has been conducted to correlate the microstructure and mechanical behavior of Sn-3.5Ag, the nature of the orientation and interface between Ag_3Sn intermetallics and the Sn-rich matrix has yet to be established. In this paper we have characterized the orientation of Ag_3Sn intermetallics, both in particle and needle-like form using OIM. We have also characterized the Ag_3Sn/Sn interface using high-resolution transmission electron microscopy (HRTEM).

Table I. Crystallographic Information for Sn and Ag_3Sn Constituents

Phase	Crystal Structure (Space Group)	Lattice Parameters (nm)
Sn	Tetragonal ($I4_1/mmm$)	$a = b = 0.5632$, $c = 0.3182$
Ag_3Sn	Orthorhombic (Pmmn)	$a = 0.5968$, $b = 0.4780$, $c = 0.5184$

MATERIALS AND EXPERIMENTAL PROCEDURE

High-purity cast ingots of Sn-3.5wt.%Ag solder were used in this study. The ingots were machined into rectangular blanks and reflowed in an aluminum mold coated with graphite. The specimens were heated to 240°C (approximately 20°C above the eutectic melting point of the alloy), held for 40 s, and cooled either by water quenching (24°C/s) or furnace cooling (0.1°C/s). Samples for OIM were subsequently aged at 175°C for 100 h to produce large Ag_3Sn particles (>2 μm) that would be easily resolvable during OIM. The microstructure of

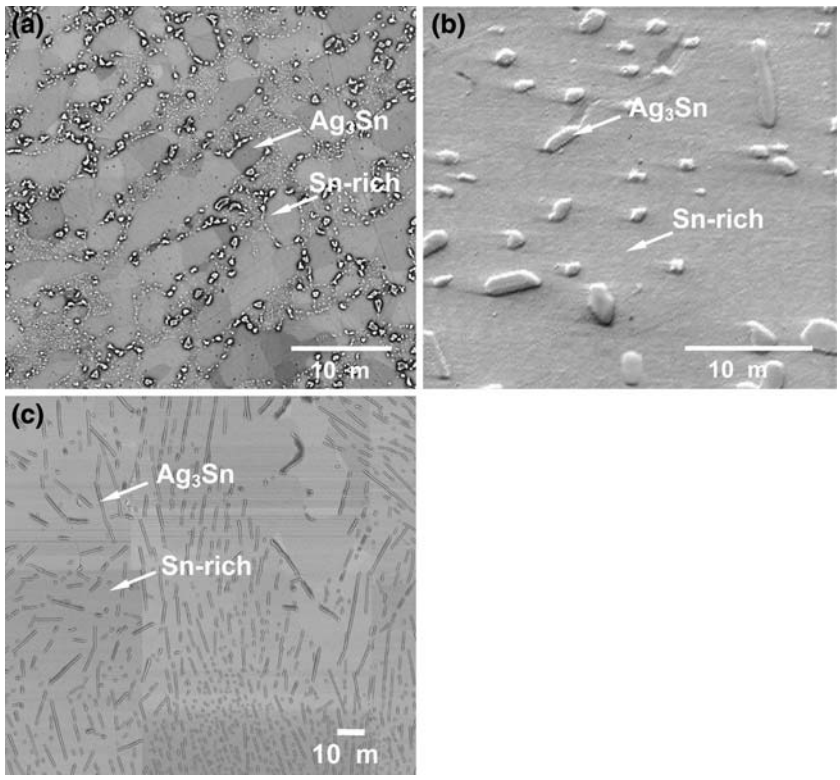

Fig. 1. Micrographs of the (a) water-cooled, (b) water-cooled aged, and (c) furnace-cooled Sn-3.5Ag solder microstructures highlighting the varying size and morphology of the Ag_3Sn intermetallics.

furnace-cooled Sn-3.5Ag[6–8] consisted of needle-like Ag_3Sn dispersed in Sn.

Specimens were sectioned from the center of the bars and polished to a 0.05 μm colloidal silica finish. OIM analysis was conducted using a Philips FEI XL30 environmental scanning electron microscope (Philips, Briarcliff Manor, NY) equipped with an electron backscatter diffraction (EBSD) system. Identification of the phases was carried out using both OIM and energy-dispersive spectroscopy (EDS). The compositions, lattice parameters, and crystal structures for Sn and Ag_3Sn are given in Table I. A large number of the Ag_3Sn intermetallic particles/needles as well as the surrounding Sn matrix were analyzed. The analysis of the orientation relationship was conducted using EDAX/TSL OIM 4 analysis software (AMETEK, Draper, UT). Neighbor orientation correlations were conducted on the OIM datasets. This operation matches the orientation of a point to its neighbor's orientation depending on the number of neighbors having the same orientation based upon a confidence index (CI) >0.2. The relative misorientation angles for the Ag_3Sn particles with respect to the Sn matrix were quantified to determine whether any preferred orientation was present.

To further investigate the interface characteristics between Ag_3Sn intermetallics and Sn, transmission electron microscopy (TEM) was conducted on the bulk unaged, water-cooled Sn-3.5Ag alloy. Samples were prepared by polishing 3-mm diameter disks to ~100 μm thickness, dimpling, and ion milling. Ion milling was conducted using a liquid-nitrogen-cooled stage to minimize sample heating, at 3.5 keV and a milling angle of 14 deg. Microstructure characterization was conducted on a JEOL 4000 EX microscope (JEOL Ltd., Tokyo, Japan), at an operating voltage of 400 keV.

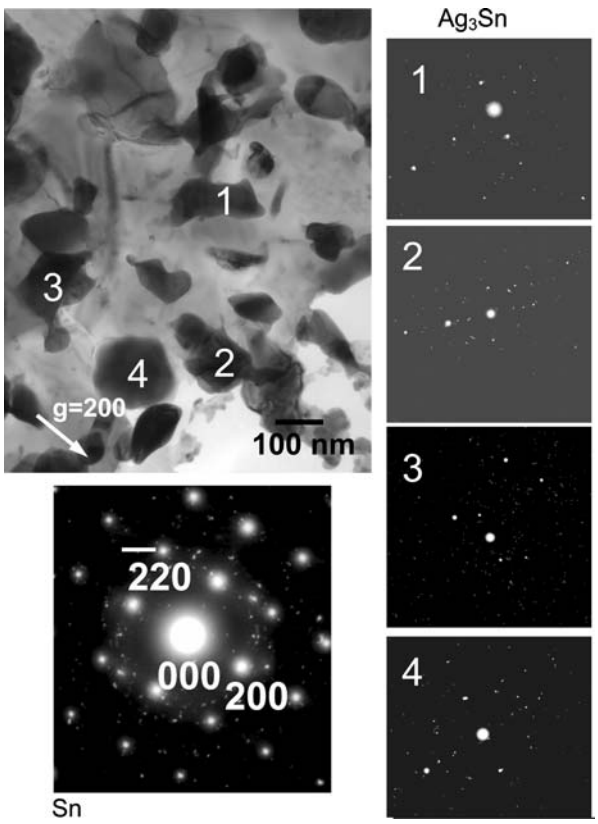

Fig. 2. Bright-field TEM image and a set of diffraction patterns obtained from a Sn-3.5Ag sample. Although the Sn matrix has a fixed orientation ⟨001⟩, the Ag_3Sn particles seem to be randomly oriented.

RESULTS AND DISCUSSION

The Sn-3.5Ag microstructure consists of Ag_3Sn intermetallics in a Sn-rich matrix.[29] The Ag_3Sn particle size and morphology were very different for the two processing conditions, as shown in Fig. 1. Water cooling resulted in nonequilibrium solidification, and produced fine microstructures consisting of Sn dendrites decorated by a eutectic mixture of finely dispersed Ag_3Sn in Sn. Near-eutectic microstructures were observed after furnace cooling, with the microstructure consisting of needle-like Ag_3Sn dispersed in Sn. For both water-cooled and water-cooled aged specimens the Ag_3Sn morphology was spherical in nature. These particles varied in size between ~300 nm and 3 to 10 μm. The furnace-cooled microstructure was much coarser, consisting of needle-like Ag_3Sn intermetallics on the order of 7 to 20 μm in length.

The nature of the Ag_3Sn/Sn interface was first characterized by TEM. The orientations of several Ag_3Sn particles were compared using bright-field imaging along a specific Sn orientation. A comparison of the individual Ag_3Sn particle orientations relative to a several specific Sn zone axes, as well as the interface between individual particles and the Sn-rich matrix, were investigated. Figure 2 shows a bright-field image of a specimen with the Sn matrix

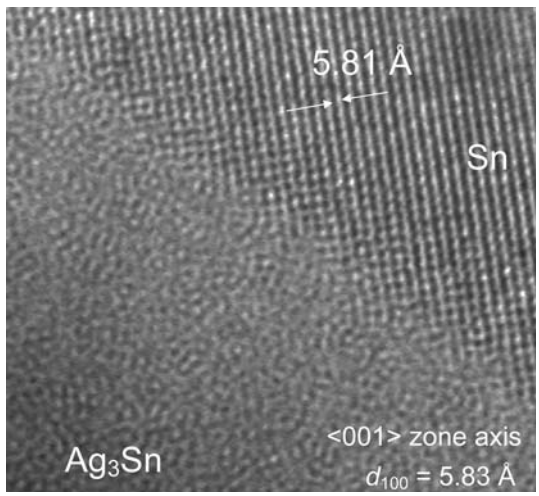

Fig. 3. HRTEM image of the Sn/Ag_3Sn interface, where the Sn grain is tilted along the ⟨001⟩ zone axis. The interface appears to be incoherent.

tilted along the ⟨001⟩ zone axis. The diffraction patterns for several Ag_3Sn intermetallics are also shown. The TEM results show that the particles have a random distribution for a given matrix orientation. This is further confirmed by OIM analysis, as discussed below. This suggests that the interface between the Sn and Ag_3Sn is likely incoherent. The inference that the Ag_3Sn/Sn interface is incoherent is reasonable considering that the lattice mismatch can be as high as 87% (i.e. along the a-axis of Ag_3Sn and the c-axis of Sn). The incoherency of the interface has implications for the creep behavior of these solders, and corroborates the findings of dislocation climb controlled by dislocation detachment from the incoherent particles.[8–10,13] Figure 3 shows a high-resolution TEM image of the Ag_3Sn and Sn interface, with the Sn matrix tilted along the ⟨001⟩ zone axis. A clear image of the atomic arrangement can be seen in the Sn. However, no lattice fringes or coincidence sites can be seen at the interface or in the Ag_3Sn particle, respectively, indicating no preferred crystallographic relationship at the interface.

OIM analysis also supported the finding of no preferred orientation relationship between Ag_3Sn particles and the Sn matrix. Figure 4 shows the SEM micrograph, phase map and [100] inverse pole figure maps of Sn and Ag_3Sn for bulk Sn-3.5Ag solder alloy aged at 175°C for 100 h. The microstructure of the Sn-3.5Ag alloy consists of a eutectic of spherical Ag_3Sn intermetallics in a Sn-rich matrix. The phase map shows that the Sn-rich matrix consists of large Sn grains that contain Ag_3Sn intermetallics that appear to be randomly oriented. The orientation of the Ag_3Sn also appears to be random over different Sn grain orientations. To verify that the Ag_3Sn intermetallics were truly randomly dispersed in the Sn-rich matrix, the misorientation angle distribution of the Ag_3Sn particles was measured, as shown in Fig. 5. It is clear from the misorientation distribution that this is a random array of particles and there is no preferred orientation relationship between Ag_3Sn and the Sn-rich matrix.

Interestingly, during solidification of the furnace-cooled specimens, the needle-like Ag_3Sn appears to be oriented in several different colonies, as shown in Fig. 6a. A similar OIM analysis was conducted on the furnace-cooled microstructure. Figure 6b shows a micrograph and subsequent phase map within a given colony. Here, within a colony there appears to be a preferred orientation of Ag_3Sn particles relative to the Sn matrix. To further verify this, a point scan analysis of the misorientation angle between Ag_3Sn and Sn was conducted in several colonies.

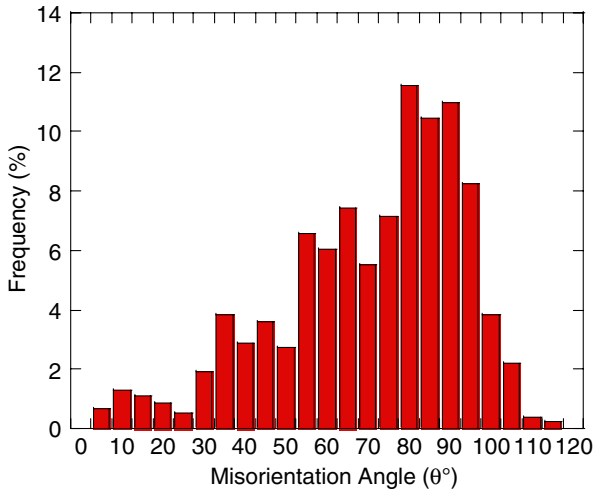

Fig. 5. Misorientation angle distribution for Ag_3Sn intermetallics in Sn-3.5Ag.

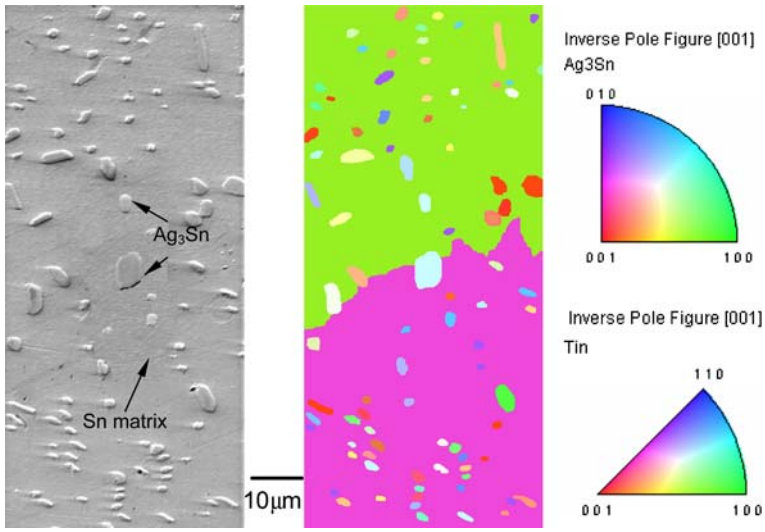

Fig. 4. SEM image and corresponding orientation map for a Sn-3.5Ag specimen. For a given Sn grain orientation, the Ag_3Sn particles seem to be randomly oriented.

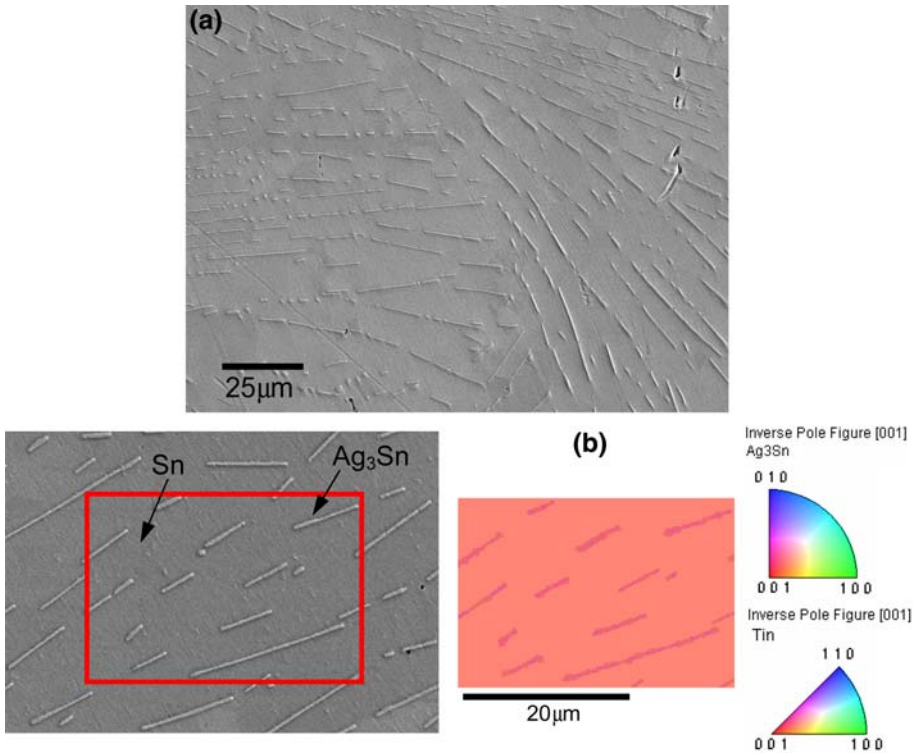

Fig. 6. (a) Furnace-cooled Sn-3.5Ag solder microstructure showing different colonies of Ag_3Sn particles; (b) phase map within a given colony showing a similar orientation between individual Ag_3Sn.

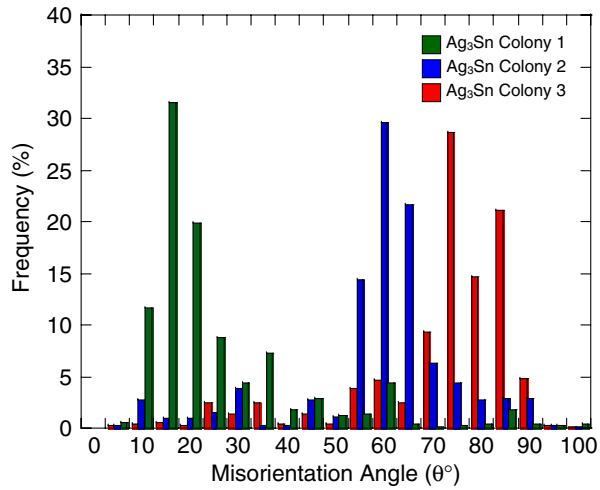

Fig. 7. Misorientation angle distribution for Ag_3Sn intermetallics in furnace-cooled Sn-3.5Ag highlighting the preferred misorientation angle within a given colony.

The misorientation angle distribution of three major colonies is shown in Fig. 7. Each colony had a unique orientation angle of Ag_3Sn needles misorientation angle distribution of Ag_3Sn particles relative to the Sn matrix. Therefore, is it clear that the Ag_3Sn needles grow along a given crystallographic orientation, which is given by the smallest misfit strain between the Ag_3Sn crystal and the Sn grains. This is likely between the a-axes, where lattice mismatch is the lowest at approximately 6%. It should be noted that, while the needles seem to be oriented in the same direction, for a given colony, this two-dimensional analysis only provides orientation information relative to the viewing plane. A full three-dimensional analysis would be required to obtain the true orientation of the needles.

From this analysis it is apparent that there is no orientation relationship between the spherical Ag_3Sn particles formed during water cooling and Sn, but there seems to be an orientation relationship between the Ag_3Sn needles and Sn matrix. In the water-cooled material, the Ag_3Sn particles undergo heterogeneous nucleation and minimal growth. The heterogeneous nucleation likely leads to the random orientation observed for the particles. In the furnace-cooled specimens, however, the Ag_3Sn particles have ample time for growth to occur. As mentioned previously, this growth is likely along orientations that reduce the strain energy, and thus results in a preferred orientation relationship with the Sn matrix.

CONCLUSIONS

The nature of the Ag_3Sn/Sn interface in a Sn-3.5Ag solder was studied using orientation imaging microscopy (OIM) and transmission electron microscopy (TEM). OIM and conventional TEM showed that, for a given orientation of the Sn

matrix, the Ag_3Sn particles do not have a preferred orientation in water-cooled samples containing spherical Ag_3Sn particles. The needle-like Ag_3Sn formed during furnace cooling appear to have a preferred orientation within separate Sn colonies. The interface between Sn and Ag_3Sn is incoherent, as confirmed by high-resolution TEM analysis. The fine distribution of randomly orientated incoherent Ag_3Sn particles has implications for the strengthening mechanisms of the solder, particularly under creep loading where dislocation climb over the Ag_3Sn particles takes place.

ACKNOWLEDGEMENTS

The authors gratefully acknowledge financial support for support of this research from the National Science Foundation under Contract #DMR-0092530 (Drs. H. Chopra, S. Ankem, B. MacDonald, and K.L. Murty, Program Managers).

REFERENCES

1. D.R. Frear and P.T. Vianco, *Metall. Mater. Trans. A* 25, 1509 (1994).
2. S. Kang and A.K. Sarkhel, *J. Electron. Mater.* 23, 701 (1994).
3. J. Glazer, *Int. Mater. Rev.* 40, 65 (1995).
4. W.J. Plumbridge and C.R. Gagg, *J. Mater. Des. Appl.* 214, 153 (2000).
5. M. Abtew and G. Selvaduray, *Mater. Sci. Eng.* 27, 95 (2000).
6. F. Ochoa, J.J. Williams, and N. Chawla, *J. Electron. Mater.* 32, 1414 (2003).
7. F. Ochoa, J.J. Williams, and N. Chawla, *JOM* 55, 56 (2003).
8. F. Ochoa, X. Deng, and N. Chawla, *J. Electron. Mater.* 33, 1596 (2004).
9. M. Kerr and N. Chawla, *Acta Mater.* 52, 4527 (2004).
10. M. Kerr and N. Chawla, *JOM* 56, 50 (2004).
11. R.S. Sidhu and N. Chawla, *Mater. Charac.* 52, 225 (2004).
12. R.S. Sidhu and N. Chawla, *Scripta Mater.* 54, 1627 (2006).
13. R.S. Sidhu, X. Deng, and N. Chawla, *Metall. Mater. Trans. A* (2007, in press).
14. C. Kuo-Ning, P. Chih-Tang, C.T. Kuo, T. Ku, and K. Chang, *Microelectron. Rel.* 46, 523 (2006).
15. M. He, Z. Chen, and G. Qi, *Metall. Mater. Trans. A* 36, 65 (2005).
16. X. Deng, R.S. Sidhu, P. Johnson, and N. Chawla, *Metall. Mater. Trans. A* 36, 55 (2005).
17. I. Dutta, C. Park, and S. Choi, *Mater. Sci. Eng. A* 379, 401 (2004).
18. B. Yeung and J. Jin-Wook, *J. Mater. Sci. Lett.* 21, 723 (2002).
19. H. Rhee, K.N. Subramanian, and A. Lee, *J. Mater. Sci.: Mater. Electron.* 16, 169 (2005).
20. W.P. Vellinga, M.A. Matin, E.W.C Coenen, and M.G.D Geers, *Scripta Mater.* 53, 927 (2005).
21. M.A. Matin, W.P. Vellinga, and M.G.D. Geers, *Mater. Sci. Eng. A* 431, 166 (2006).
22. M.A. Matin, W.P. Vellinga, and M.G.D. Geers, *Mater. Sci. Eng. A* 445–446, 73 (2007).
23. A.U. Telang and T.R. Bieler, *Scripta Mater.* 52, 1027 (2005).
24. A.U. Telang, T.R. Bieler, J.P. Lucas, K.N. Subramanian, L.P. Lehman, Y. Xing, and E.J. Cotts, *J. Electron. Mater.* 33, 1412 (2004).
25. A.U. Telang and T.R. Bieler, *Diff. Defect Data B: Sol. State Phen.* 105, 219 (2005).
26. V. Kumar, Z.F. Zhigang, L. Jin, and N. Dariavach, *Metall. Mater. Trans. A* 37, 2505 (2006).
27. A.U. Telang, T.R. Bieler, D.E. Mason, and K.N. Subramanian, *J. Electron. Mater.* 32, 1455 (2003).
28. A.U. Telang and T.R. Bieler, *JOM* 57, 44 (2005).
29. R.S. Sidhu and N. Chawla, *Metall. Mater. Trans. A* (2007, in press).